



Rapid crustal growth and efficient crustal recycling in the early Earth: Implications for Hadean and Archean geodynamics

Juan Carlos Rosas, Jun Korenaga*

Department of Geology and Geophysics, Yale University, P.O. Box 208109, New Haven, CT 06520-8109, USA

ARTICLE INFO

Article history:

Received 11 March 2018

Received in revised form 24 April 2018

Accepted 26 April 2018

Available online xxxx

Editor: A. Yin

Keywords:

Sm–Nd isotope systems

crust–mantle differentiation

plate tectonics

ABSTRACT

The geodynamic regime of the early Earth remains elusive, with so far proposed hypotheses ranging from stagnant lid convection to rapid plate tectonics. Available geological data are severely limited for the first two billion years of the Earth's history, and this scarcity of relevant data is often compounded by the nonuniqueness of interpretation. Here we propose that the samarium–neodymium isotope evolution, which has been suggested to be consistent with stagnant lid convection in the early Earth, may be better understood as the result of rapid crustal growth and extensive crustal recycling. We delineate the permissible scenario of crustal evolution through geochemical box modeling with a Monte Carlo sampling of the model parameter space, and our results suggest that the net growth of continental crust was complete by the end of the Hadean and that the rate of crustal recycling could have been as high as $2 - 4 \times 10^{22} \text{ kg Gyr}^{-1}$ at that time and has gradually decreased since then. Such crustal evolution yields a specific prediction for the present-day distribution of crustal formation ages, which is shown to be in remarkable agreement with a recent estimate based on the global compilation of zircon age data. The mode of subsolidus mantle convection after the putative magma ocean is probably plate tectonics, but its style could have been very different from that of contemporary plate tectonics, characterized by more voluminous magmatism and more destructive subduction.

© 2018 Elsevier B.V. All rights reserved.

1. Introduction

Reconstructing the geodynamic regime of Earth during its first two billion years is challenging due to the paucity of relevant geological data. Rocks of Archean ages are considerably less abundant than those of Proterozoic ages, and little rock has survived from the Hadean, with the mineral zircon being the primary probe for this eon. Because of the lack of decisive observational constraints, the onset of plate tectonics or, more generally, the mode of mantle convection in the early Earth remains a controversial topic (e.g., Korenaga, 2013). The operation of plate tectonics is inherently linked to the long-term CO₂ cycle, the oxygenation of the atmosphere, and the global water cycle, via subduction and volcanic degassing (e.g., Holland, 1984; Lyons et al., 2014; Korenaga et al., 2017). As these processes exert first-order control on the evolution of surface environment, resolving the geodynamic regime of the early Earth is essential if we wish to understand the evolution of the planet as a whole.

* Corresponding author.

E-mail addresses: juan.rosas@yale.edu (J.C. Rosas), jun.korenaga@yale.edu (J. Korenaga).

<https://doi.org/10.1016/j.epsl.2018.04.051>

0012-821X/© 2018 Elsevier B.V. All rights reserved.

Existing models for mantle convection in the early Earth span stagnant lid convection (e.g., O'Neill and Debaille, 2014) to rapid plate tectonics (e.g., Sleep et al., 2014). Proponents for different models employ different kinds of observations or theoretical reasoning, and given the fundamental limitation of available geological data, it is important to examine the robustness of each of these arguments. Here we focus on the samarium–neodymium (Sm–Nd) isotope evolution, which has recently been used as key supporting evidence for stagnant lid convection in the early Earth (Debaille et al., 2013; O'Neill and Debaille, 2014). Both Sm and Nd are lithophile and incompatible elements, with Nd being slightly more incompatible than Sm. The pair of these two elements is particularly attractive for tracking crust–mantle differentiation, owing to the existence of two isotope systems with vastly different decay constants: ¹⁴⁷Sm and ¹⁴⁶Sm decay into ¹⁴³Nd and ¹⁴²Nd, respectively, with the corresponding half-lives of ~106 Gyr and ~103 Myr. Whereas the ¹⁴³Nd evolution of the depleted mantle (Fig. 1a) is commonly interpreted as the result of continental crust extraction (e.g., Bennett, 2003), the ¹⁴²Nd evolution (Fig. 1b) has been suggested to reflect inefficient mantle mixing associated with stagnant lid convection (Debaille et al., 2013). The amplitude of μ_{Nd}^{142} anomalies is as high as ~20 in the early Archean, and it takes more than 1 Gyr for μ_{Nd}^{142} to be reduced to approximately zero. If

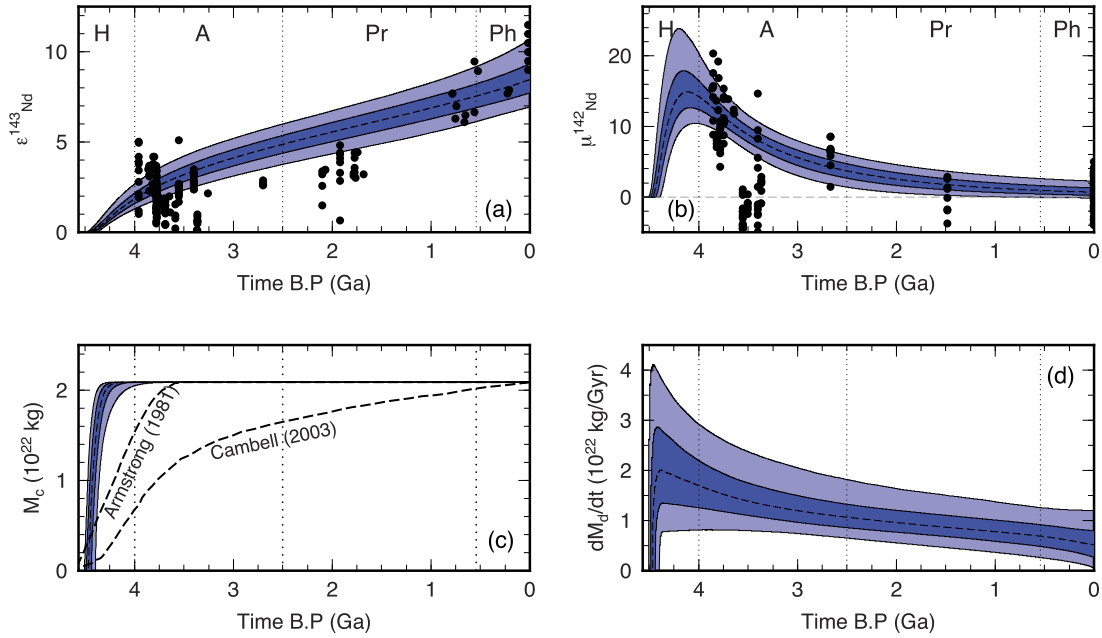


Fig. 1. (a) ^{143}Nd and (b) ^{142}Nd evolution of the depleted mantle based on published data (Baadsgaard et al., 1986; Moorbath et al., 1997; Vervoort and Blichert-Toft, 1999; Caro et al., 2006, 2017; Bennett et al., 2007; Murphy et al., 2010; Rizo et al., 2012; Jackson and Carlson, 2012; Debaille et al., 2013; Roth et al., 2014; Puchtel et al., 2016; Morino et al., 2017) as a function of time before present, from $t = 4.567$ Ga (solar system initial) to $t = 0$ (present). $\epsilon^{143}\text{Nd}(t)$ is defined as $[(^{143}\text{Nd}/^{144}\text{Nd})_t / (^{143}\text{Nd}/^{144}\text{Nd})_t^{\text{CHUR}} - 1] \times 10^4$, and $\mu^{142}\text{Nd}(t)$ as $[(^{142}\text{Nd}/^{144}\text{Nd})_t / (^{142}\text{Nd}/^{144}\text{Nd})_t^{\text{std}} - 1] \times 10^6$, where CHUR and std stand for the chondritic uniform reservoir and the terrestrial standard reference, respectively. Also shown are the results of box modeling corresponding to (c) crustal growth and (d) crustal recycling rate. Dark blue region denotes the inter-quartile range, representing the mid 50% of all successful solutions, whereas light blue region covers from the 5th to 95th percentile. Dotted line represents the median. Vertical dotted lines divide the Earth's history into the Hadean (H), the Archean (A), the Proterozoic (Pr) and the Phanerozoic (Ph). Previous models of net continental growth (Armstrong, 1981; Campbell, 2003) are also shown in (c) for comparison. (For interpretation of the colors in the figure(s), the reader is referred to the web version of this article.)

mantle mixing is responsible for this gradual decrease in $\mu^{142}\text{Nd}$, its long timescale may not be consistent with the operation of plate tectonics.

This interpretation of the ^{142}Nd evolution is, however, questionable on at least two accounts. First, inefficient mantle mixing by itself does not necessarily preclude the possibility of plate tectonics. Various kinds of geological evidence suggest that the tempo of plate tectonics was not faster in the past (Bradley, 2008; Herzberg et al., 2010; Padhi et al., 2012; Condie et al., 2015; Pehrsson et al., 2016; Korenaga et al., 2017), which could reduce the efficiency of mantle mixing substantially (Korenaga, 2006). Second, and more important, the ^{142}Nd evolution can also be interpreted as the result of crustal recycling (Caro et al., 2006, 2017; Roth et al., 2014), as opposed to mantle mixing. Between these two possibilities, the interpretation with crustal recycling has the advantage of being able to be tested against crustal age data. In this study, therefore, we choose to pursue this alternative idea in a systematic manner. As shown later, the present-day distribution of crustal formation ages, as well as the current rate of sediment subduction, provides strong support to the interpretation based on crustal recycling. The coupled ^{143}Nd and ^{142}Nd evolution indicates the occurrence of intensive crustal generation and recycling throughout the early Earth, and we will discuss the implications of such crustal evolution for Hadean and Archean geodynamics.

2. Model setup

We employ a box modeling approach to study the evolution of $\epsilon^{143}\text{Nd}$ and $\mu^{142}\text{Nd}$ in the continental crust and depleted mantle. The isotopes involved are the parent isotopes ^{147}Sm and ^{146}Sm , their radiogenic daughters ^{143}Nd and ^{142}Nd , and the non-radiogenic isotope ^{144}Nd . The initial composition of the mantle is equal to the composition of the bulk silicate Earth (BSE) (Lyubetskaya and Korenaga, 2007a). The masses of the depleted mantle and the continental crust are given by $M_m(t)$ and $M_c(t)$, respectively. The rate

of mass gained or lost by the depleted mantle is given by $\dot{M}_d(t)$ and $\dot{M}_u(t)$, respectively (overdot stands for time derivative). The net growth of the continental crust is given by $\dot{M}_c = \dot{M}_u - \dot{M}_d$. The total mass of the system is always conserved as $\dot{M}_c = -\dot{M}_m$. Continental crust growth and recycling are parameterized as

$$M_c(t) = \frac{M_c(t_p)}{1 - e^{-\kappa_g(t_p - t_s)}} \left(1 - e^{-\kappa_g(t - t_s)}\right), \quad (1)$$

and

$$\dot{M}_d(t) = R_s + \frac{R_p - R_s}{1 - e^{-\kappa_r(t_p - t_s)}} \left(1 - e^{-\kappa_r(t - t_s)}\right), \quad (2)$$

where t_s and t_p correspond to, respectively, the time when crustal growth and recycling started and the present-day (4.56 Gyr after the solar system initial). The terms R_s and R_p are the recycling rates at $t = t_s$ and $t = t_p$, respectively, and κ_g and κ_r are decay constants for crustal growth and recycling rate. Both $M_c(t)$ and $\dot{M}_d(t)$ are set to zero for $t < t_s$, and the present-day value for the crustal mass $M_c(t_p)$ is set to 2.09×10^{22} kg. By varying t_s , κ_g , κ_r , R_s , and R_p , we can test a wide range of scenarios for crustal growth and recycling. Eqs. (1) and (2) can handle only monotonic variations, but they are sufficiently flexible to allow us to reproduce the first-order features of Nd isotope evolution.

Following DePaolo (1980), the mass balance equations for the parent (j), the daughter (i'), and the reference isotope (i) in the mantle are given by

$$\begin{aligned} \dot{M}_m C_m^j + M_m \dot{C}_m^j &= \dot{M}_d C_c^j - \dot{M}_u D_j C_m^j - \lambda_j N_m^j, \\ \dot{M}_m C_m^{i'} + M_m \dot{C}_m^{i'} &= \dot{M}_d C_c^{i'} - \dot{M}_u D_i C_m^{i'} + \lambda_j N_m^j, \\ \dot{M}_m C_m^i + M_m \dot{C}_m^i &= \dot{M}_d C_c^i - \dot{M}_u D_i C_m^i, \end{aligned} \quad (3)$$

where the subscripts m and c stand for mantle and crust, C are the concentrations of the different species, D are the crustal enrichment factors, λ is the decay constant, and N is the total number of

atoms, with similar equations for the concentrations in the continental crust. The crustal enrichment factors control elemental partitioning upon the generation of new continental crust. The genesis of continental crust cannot be represented by single-stage mantle melting, and it is generally believed to involve multiple processes such as intracrustal differentiation, metasomatism, and crustal delamination. An enrichment factor should thus be regarded as an ‘effective’ parameter that quantifies the overall partitioning behavior resulting from such multiple processes.

Regarding the initial condition of μ_{Nd}^{142} , a deficit of ~ 20 observed in chondritic meteorites with respect to the terrestrial standard has been suggested to require either a super-chondritic Earth or global BSE differentiation into an early depleted reservoir and an early enriched reservoir (Boyett and Carlson, 2005). Recently, however, this deficit has been shown to be the result of the Earth having a larger component of the slow neutron-capture process (s-process) with respect to chondrites (Bouvier and Boyett, 2016; Burkhardt et al., 2016). Therefore, the initial conditions for the BSE are calculated through standard radioactive equations from the present-day isotope ratios for the CHUR and terrestrial standard (Jacobsen and Wasserburg, 1984; Boyett and Carlson, 2005; Bouvier et al., 2008; Marks et al., 2014; Sanborn et al., 2015): $(^{147}\text{Sm}/^{144}\text{Nd})_{t_0}^{\text{CHUR}} = 0.201942$, $(^{143}\text{Nd}/^{144}\text{Nd})_{t_0}^{\text{CHUR}} = 0.506687$, $(^{146}\text{Sm}/^{144}\text{Nd})_{t_0}^{\text{CHUR}} = 0.000336$, and $(^{142}\text{Nd}/^{144}\text{Nd})_{t_0}^{\text{std}} = 1.141511$, where t_0 denotes the solar system initial, and $(^{146}\text{Sm}/^{144}\text{Nd})_{t_0}^{\text{CHUR}}$ is calculated from $(^{146}\text{Sm}/^{144}\text{Sm})_{t_0}^{\text{CHUR}}$ and $(^{144}\text{Sm}/^{144}\text{Nd})_{t_0}^{\text{CHUR}}$.

Our modeling strategy is to focus on the secular evolution of the average composition of the depleted component in the mantle, and we do not attempt to model isotopic variability in the mantle, for the following two reasons. First, it is difficult to reliably estimate the isotopic variability of source mantle for igneous rocks found in continental setting, because of various possibilities of crustal contamination. When judging whether a piece of continental rock is ‘mantle-derived’ or not, one of the common criteria is that its ε_{Nd} is sufficiently high, so published constraints on the Nd isotope evolution of the depleted mantle are already biased to the depleted end-member (commonly referred to as the depleted MORB-source mantle, where MORB stands for mid-ocean-ridge basalts (Zindler and Hart, 1986)). The problem is compounded for ancient rocks because metamorphic changes to Sm/Nd ratios make it difficult to accurately determine the initial Nd isotopic composition. Second, modeling isotopic variability involves more assumptions than modeling average compositions (Allegre and Lewin, 1995; Caro et al., 2006; Roth et al., 2014). The processes assumed for the source of variability in the dispersion modeling are unlikely to be exhaustive, and validating the assumptions made for mixing processes is difficult because the reality of mantle mixing is still largely unresolved, owing to the lack of accurate understanding of rock rheology (Manga, 1996; Korenaga and Karato, 2008; Jain et al., 2018).

Our model has ten free parameters in total: five parameters to describe crustal growth and recycling (t_s , κ_g , κ_r , R_s , and R_p), initial and final enrichment factors for Sm and Nd ($D_{\text{Sm}}(t_s)$, $D_{\text{Sm}}(t_p)$, $D_{\text{Nd}}(t_s)$, and $D_{\text{Nd}}(t_p)$); enrichment factors vary linearly between the initial and final values), and the mass fraction of the depleted mantle with respect to the whole mantle, f_m . The *a priori* ranges for these parameters are set as follows: (4.37, 4.51) Ga for t_s , (−1, 30) Gyr^{-1} for κ_g , (−3, 3) Gyr^{-1} for κ_r , (0, 5×10^{22}) kg Gyr^{-1} for R_s and R_p , (1, 50) for the enrichment factors, with the condition that $D_{\text{Sm}} < D_{\text{Nd}}$ all the time, and (0.1, 0.9) for f_m . The range of t_s corresponds to the oldest terrestrial zircon (Valley et al., 2014) and the separation of the silicate reservoirs due to the Moon-forming event (Barboni et al., 2017). The depleted mantle in our box model does not necessarily correspond to the shallow part of the convecting mantle; it is more of abstract nature, representing the fraction

of the mantle that is chemically complementary to the continental crust, and it may be physically distributed throughout the mantle. The volume of this depleted component is time-independent as in the original formulation of DePaolo (1980), and unlike some of previous box modeling studies (e.g., McCulloch and Bennett, 1994), its interaction with the more primitive component is not considered; doing so would add at least one more free parameter, thereby increasing the nonuniqueness of box modeling. The rarity of the early Archean and Hadean rocks that exhibit positive Nd isotopic anomalies may indicate that the volume of the depleted mantle was considerably smaller in the early Earth, but such rarity may simply have resulted from the combined effects of crustal recycling and reworking over the Earth’s history. Our modeling strategy is to adopt something simple (the time-independent depleted mantle component) yet sufficiently flexible (our parameterization of crustal growth and recycling) and then validate our assumptions by comparing model predictions with independent constraints on crustal evolution.

3. Results

We conducted the Monte Carlo sampling of the aforementioned parameter space using the Mersenne Twister (Matsumoto and Nishimura, 1998) as a pseudo-random number generator, with the total number of iterations up to 4.5×10^7 . The solutions were first screened by their ability to reproduce the crust and mantle concentrations of Sm and Nd at the present day: C_{Sm} between 2.7 and 5.1 ppm and C_{Nd} between 14 and 26 ppm for the crust, and C_{Sm} between 0.24 and 0.47 ppm and C_{Nd} between 0.58 and 1.45 ppm for the depleted mantle (Korenaga, 2009). With this screening, the number of the valid solutions was reduced to $\sim 8 \times 10^6$. These solutions were then further screened using their deviations from the observed ^{143}Nd and ^{142}Nd evolution, as follows. We define the total misfit, M , as

$$M = \log_{10} \left[\frac{(\sigma_\varepsilon - \min(\sigma_\varepsilon))^2}{\Delta_\varepsilon^2} + \frac{(\sigma_\mu - \min(\sigma_\mu))^2}{\Delta_\mu^2} \right], \quad (4)$$

where σ_ε is given by

$$\sigma_\varepsilon = \left\{ \sum_{k=1}^n \frac{1}{n} \left[\varepsilon_{\text{Nd}}^{143}(t_k) - (\varepsilon_{\text{Nd}}^{143})_k \right]^2 \right\}^{1/2}, \quad (5)$$

with $\varepsilon_{\text{Nd}}^{143}(t_k)$ denoting model prediction at $t = t_k$, and σ_μ is defined similarly with μ_{Nd}^{142} . A pair of t_k and $(\varepsilon_{\text{Nd}}^{143})_k$ or $(\mu_{\text{Nd}}^{142})_k$ is called an anchor point, and we used six anchor points for σ_ε : (3.96, 2.5), (3.75, 1.97), (3.4, 2.88), (1.92, 3.95), (0.625, 7.75), and (0, 10), and five anchor points for σ_μ : (3.80, 15), (3.4, 9), (2.66, 5), (1.48, 0), and (0, 0) (all ages are in Ga). These anchor points were chosen to select the solutions that can mimic the gross behavior of Nd isotope evolution. Whereas recent studies on Archean and Hadean terranes suggest that negative μ_{Nd}^{142} anomalies may be more common than the positive ones (e.g., O’Neil et al., 2012; Roth et al., 2014; Caro et al., 2017; Morino et al., 2017), focusing on the positive side of the μ_{Nd}^{142} anomalies is consistent with our modeling strategy of the depleted mantle component. The term $\min(\sigma_{\varepsilon,\mu})$ denotes the minimum value of $\sigma_{\varepsilon,\mu}$ among all solutions, and as the amplitude of μ_{Nd}^{142} variation is about twice as large as that of $\varepsilon_{\text{Nd}}^{143}$ variation, we set $\Delta_\varepsilon = 1$ and $\Delta_\mu = 2$ to balance different isotope constraints. A solution with the total misfit less than 0.5 appears to provide a reasonable fit to the observed Nd evolution, and the number of such solutions is $\sim 2 \times 10^4$. The statistical representation of this successful Monte Carlo ensemble is given in Figs. 1 and 2.

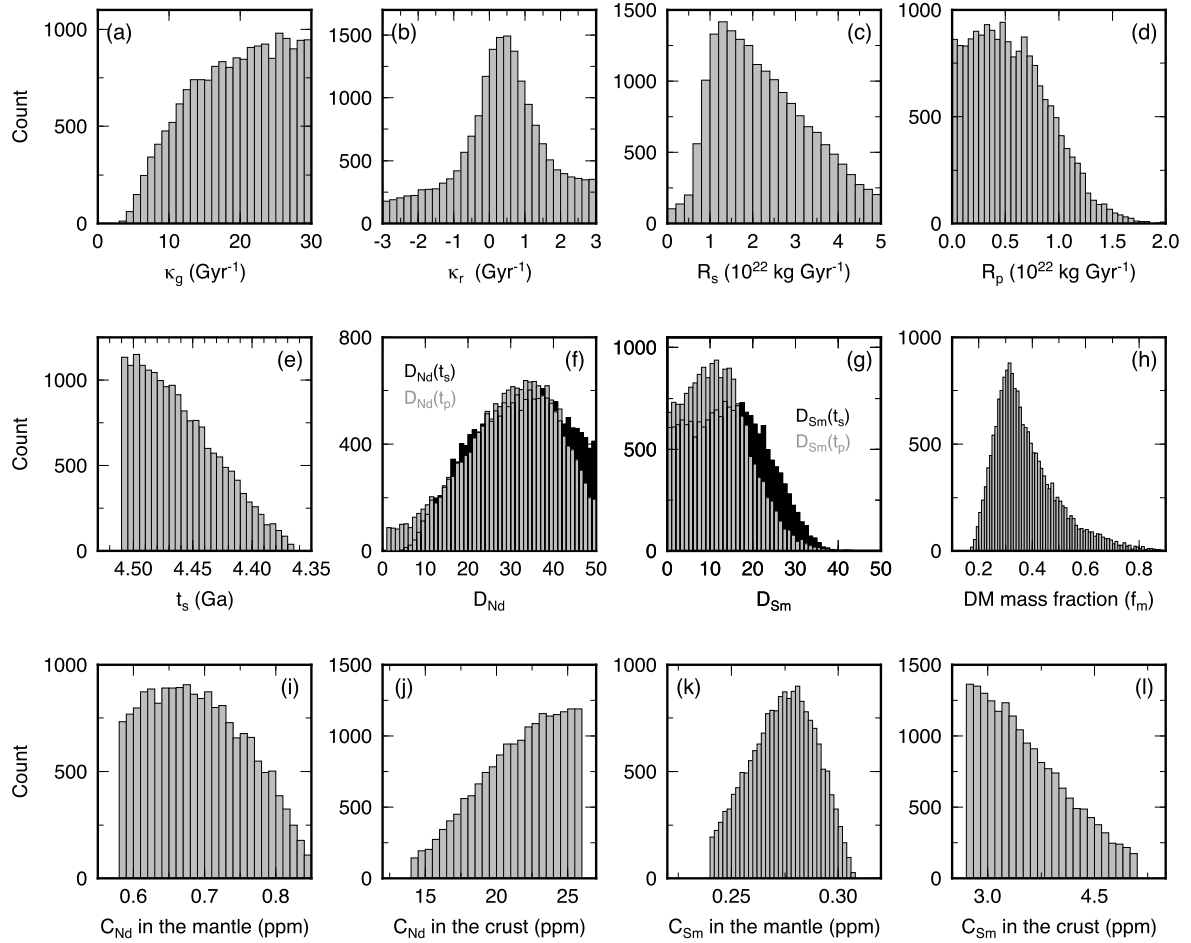


Fig. 2. The a posteriori distributions of input model parameters and some model variables, based on $\sim 2 \times 10^4$ successful Monte Carlo solutions. (a) Decay constant for continental growth, (b) decay constant for crustal recycling, (c) initial recycling rate, (d) present-day recycling rate, (e) onset time for crustal generation and recycling, (f) initial (black) and present-day (gray) crustal enrichment factors for Nd, (g) crustal enrichment factors for Sm, (h) mass fraction of the depleted mantle, (i) Nd concentration in the depleted mantle, (j) Nd concentration in the continental crust, (k) Sm concentration in the depleted mantle, and (l) Sm concentration in the continental crust. The concentrations in (i)–(l) are all at the present day.

For crustal growth, κ_g is varied from -1 to 30 Gyr^{-1} , covering from linear crustal growth to nearly instantaneous growth. For crustal recycling, R_s and R_p are varied from 0 to $5 \times 10^{22} \text{ kg Gyr}^{-1}$, to model both increasing and decreasing trends, and κ_r is varied from -3 Gyr^{-1} to 3 Gyr^{-1} so that the temporal evolution of recycling rate can be either concave upward or downward. Successful cases are, however, all characterized by rapid crustal growth ($\kappa_g > \sim 4 \text{ Gyr}^{-1}$; Figs. 1c and 2a) and high recycling rate in the Hadean ($R_s \sim 2 \times 10^{22} \text{ kg Gyr}^{-1}$), with a gradual fourfold decrease over the Earth's history (Fig. 1d). Rapid crustal growth is necessary to achieve the high μ_{Nd}^{142} values at $\sim 4 \text{ Ga}$, and intensive crustal recycling must occur concurrently to reproduce its steady decrease over the Archean (Fig. 1b). The extent of crustal recycling should wane subsequently to match the overall $\varepsilon_{\text{Nd}}^{143}$ evolution (Fig. 1a). Within the *a priori* range of the growth start time t_s (4.37 to 4.51 Ga), the successful solutions prefer the earlier onset of crustal genesis (Fig. 2e), and this is consistent with the suggestion that the Earth had a continental crust already at 4.4 Ga (Mojzsis et al., 2001; Wilde et al., 2001; Harrison et al., 2005). The crustal enrichment factors are only loosely constrained at ~ 30 – 40 for Nd and ~ 10 – 20 for Sm, and no major temporal change seems to be required for them (Fig. 2f, g). The mass fraction of the depleted mantle peaks at ~ 0.3 (Fig. 2h), similar to what classical box modeling studies suggest (e.g., Jacobsen and Wasserburg, 1979), but its probability distribution is rather diffuse, with the 90% confidence limit ranging from 0.23 to 0.62, reflecting the imprecise

nature of geochemical mass balance (Allegre et al., 1983; Lyubetskaya and Korenaga, 2007b). By the nature of our screening, model predictions for the present-day Sm and Nd concentrations in the crust and mantle are all within the acceptable ranges (Figs. 2i–l).

To better understand how crustal growth and recycling are constrained by the coupled ^{143}Nd and ^{142}Nd evolution, a few illustrative examples are given in Fig. 3. The comparison of three different growth models, with the median recycling rate shown in Fig. 1d (dotted line), indicates that rapid crustal growth is constrained mostly by the ^{142}Nd evolution (Fig. 3, top row). Because ^{146}Sm was effectively extinct by the end of the Hadean, the mantle has to be substantially depleted in the early Hadean to explain the high μ_{Nd}^{142} values in the early Archean (Fig. 3c). As the half-life of ^{147}Sm is much longer than the age of the Earth, on the other hand, the ^{143}Nd evolution is not very sensitive to the details of crustal growth (Fig. 3b). By contrast, the long-term ^{143}Nd evolution is sensitive to the temporal evolution of crustal recycling (Fig. 3, bottom row). Using the median growth curve shown in Fig. 1c (dotted line), three kinds of crustal recycling are compared: a time-decaying recycling rate, and two constant recycling rates of $1.2 \times 10^{22} \text{ kg Gyr}^{-1}$ and $0.1 \times 10^{22} \text{ kg Gyr}^{-1}$ (Fig. 3d). The case with the low recycling rate results in a mantle that is simply too depleted, and neither ^{143}Nd nor ^{142}Nd evolution can be reproduced. The observed decrease in μ_{Nd}^{142} during the Archean demands substantial crustal recycling but is relatively insensitive to how recycling varies with time (Fig. 3f). It

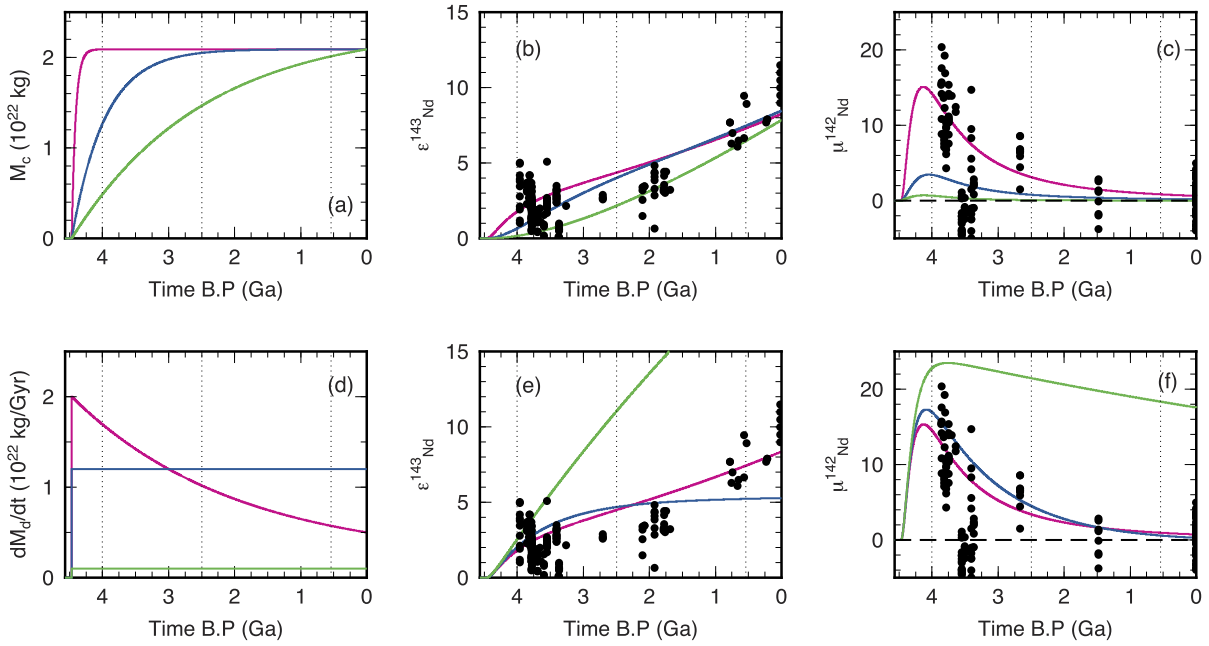


Fig. 3. Top row: effect of crustal growth on the Nd isotope evolution. (a) Crustal growth functions using $\kappa_g = 0.5$ (green), 2.0 (blue), and 17 (red). (b) Corresponding evolution of $\epsilon_{\text{Nd}}^{143}$, with the median solution for the recycling rate (Fig. 1d). (c) Same as (b), but for μ_{Nd}^{142} . Bottom row: effect of crustal recycling. (d) Recycling rate functions using $R_s = 2.0 \times 10^{22}$ kg Gyr $^{-1}$, $R_p = 0.5 \times 10^{22}$ kg Gyr $^{-1}$, and $\kappa_r = 0.5$ (red), $R_s = R_p = 1.2 \times 10^{22}$ kg Gyr $^{-1}$ and $\kappa_r = 0$ (blue), and $R_s = R_p = 0.10 \times 10^{22}$ kg Gyr $^{-1}$ and $\kappa_r = 0$ (green). (e) Corresponding evolution of $\epsilon_{\text{Nd}}^{143}$, with the median solution for crustal growth (Fig. 1c). (f) Same as (e), but for μ_{Nd}^{142} . All models share the following parameters: $t_s = 4.51$ Ga, $D_{\text{Nd}}(t_s) = 35$, $D_{\text{Nd}}(t_p) = 45$, $D_{\text{Sm}}(t_s) = 20$, $D_{\text{Sm}}(t_p) = 25$, and $f_m = 0.35$.

can be seen that the ^{143}Nd evolution is what dictates the reduced recycling rate in the post-Archean era (Fig. 3e). Modeling results suggest that the 90% confidence limit for the present-day recycling rate is $0.1\text{--}1.2 \times 10^{22}$ kg Gyr $^{-1}$ (Fig. 1d), which encompasses geological estimates for the present-day crustal recycling rate based on sediment subduction ($2.5\text{--}3.2$ km 3 yr $^{-1}$ (Scholl and von Huene, 2007; Stern and Scholl, 2010), which is equivalent to $0.7\text{--}0.9 \times 10^{22}$ kg Gyr $^{-1}$ with a crustal density of 2700 kg m $^{-3}$). It is notable that our box modeling was able to reproduce an acceptable present-day recycling rate without using such a constraint in the modeling.

Our preferred model of continental growth suggests that, by the end of the Hadean, the continental crust was volumetrically equivalent to the present day (Fig. 1c). It does not mean, however, that the Hadean crust should occupy much of the present-day continental crust because the recycling of crust into the mantle was also more efficient in the early Earth (Fig. 1d). This can be readily quantified by calculating the present-day distribution of crustal formation ages from the box modeling results as follows. First, we denote the mass distribution of crustal formation ages at some time t by $m(t, \tau)$, where τ is the formation age. This distribution and the continental mass are related as

$$\int_0^t m(t, \tau) d\tau = M_c(t). \quad (6)$$

In our box modeling, the continental crust is treated as a single uniform reservoir, so when the crust is recycled at the rate of $\dot{M}_d(t)$, all the crust is affected uniformly, independent of formation ages. The temporal evolution of $m(t, \tau)$ with this age-independent recycling may be expressed as

$$\frac{\partial m(t, \tau)}{\partial t} = \dot{M}_u(t) \delta(t - \tau) - \frac{\dot{M}_d(t)}{M_c(t)} m(t, \tau), \quad (7)$$

where $\delta(t)$ is the Dirac delta function. The present-day distribution $m(t_p, \tau)$ can then be calculated by integrating the above differen-

tial equation, starting at $t = 0$. Finally, the present-day cumulative distribution of formation ages, $F(\tau)$, is calculated as

$$F(\tau) = \frac{1}{M_c(t_p)} \int_0^\tau m(t_p, \tau') d\tau'. \quad (8)$$

Note that the age-independent recycling here does not mean that recycled materials at any given time contain all formation ages equally. As seen in Eq. (7), the crust is recycled in proportion to $m(t, \tau)$; for example, if the crust with the formation age of 3 Ga is twice as abundant than that with the formation age of 4 Ga, such proportionality is directly reflected in recycled materials. Also, it is important to understand that $m(t, \tau)$ represents the distribution of ‘original’ crustal formation ages, so the ‘apparent’ ages of recycled materials can deviate to younger ages because of crustal reworking. Some authors argue against crustal recycling in the early Earth by noting that all <3.5 Ga terrigenous sediments in active margins and continental settings have Nd and Hf model ages younger than 3.5 Ga (e.g., Iizuka et al., 2017), but such observation does not preclude the recycling of >3.5 Ga materials because those model ages are likely to have been affected by crustal reworking (Korenaga, 2018).

The present-day distribution of crustal formation ages computed from our modeling results shows that only $\sim 10\%$ and $\sim 30\%$ of the present-day crust are originally formed during the Hadean and the Archean, respectively (Fig. 4). More important, the formation age distribution based on the Sm–Nd isotope systems is in remarkable agreement with that estimated from the global compilation of zircon age data (Korenaga, 2018). The convergence of these two entirely independent estimates, based on different geochemical data as well as different methods, is encouraging, suggesting that the modeling strategy based on crustal recycling allows us to probe correctly the origin of the observed Nd isotope evolution. As indicated in Fig. 4, the difference between the formation age distribution and the surface age distribution reflects the effect of crustal reworking, i.e., the remobilization of preexisting crust by partial melting or erosion and sedimentation. About 10% of present crust

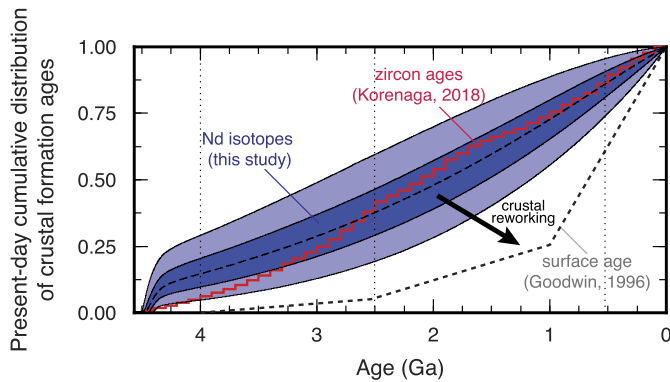


Fig. 4. Present-day cumulative distribution of crustal formation age, as computed from crustal growth (Fig. 1c) and crustal recycling (Fig. 1d). The cumulative distribution is normalized by the present-day continental mass. The meaning of blue shadings are the same as in Fig. 1. An estimate based on the global compilation of zircon age data (Korenaga, 2018) (red) as well as the present-day surface age distribution (gray dotted) (Goodwin, 1996) are also shown for comparison. Difference between the distributions of formation ages and surface ages signifies the effect of crustal reworking.

having already existed in the Hadean may appear too high, given that the documented occurrence of pre-3.8 Ga rocks is rather rare on Earth. However, older rocks are subject to a greater likelihood of being affected by crustal reworking, and the most of the Hadean crust could have been sourced for younger crust (e.g., O’Neil and Carlson, 2017).

4. Discussion

Our modeling results are characterized by rapid crustal growth in the early Earth and gradually declining crustal recycling, both of which are qualitatively similar to the model of Armstrong (1981). In the Armstrong model, the continental crust does not achieve the present-day mass before ~ 3.6 Ga, but this part of his model is largely speculative and not observationally constrained. The model of Campbell (2003) is based on the secular evolution of Nb/U of the mantle, the original data of which do not demand notable crustal growth since the early Archean, and the diminishing Hadean crustal mass in his model is based mostly on the scarcity of Hadean zircons, which can instead be explained by efficient crustal recycling as our modeling results indicate and also by crustal reworking (Korenaga, 2018). Some authors argue for subdued crustal recycling in the Hadean based on the preservation of Hadean precursor in Archean rocks (Caro et al., 2017), but such preservation by itself does not quantify the efficiency of crustal recycling. Even with the recycling rate several times greater than the present-day rate (Fig. 1d), a fraction of the crustal material originally produced in the Hadean can remain on the Earth’s surface to the present (Fig. 4).

Crustal recycling in the early Earth is estimated as $\sim 2 \times 10^{22}$ kg Gyr $^{-1}$ and can be as high as $\sim 4 \times 10^{22}$ kg Gyr $^{-1}$ (Fig. 1d). Interestingly, the same level of recycling has also been suggested by the modeling of isotopic dispersion (Caro et al., 2006; Roth et al., 2014); with the crustal mass of $\sim 2 \times 10^{22}$ kg, the crustal residence time of 0.5–0.75 Gyr suggested by these studies is equivalent to the recycling rate of $2.7\text{--}4 \times 10^{22}$ kg Gyr $^{-1}$, which is considerably higher than the present-day rate of recycling. As mentioned earlier, the validity of dispersion modeling is uncertain, but arriving at a similar conclusion with different modeling assumptions may attest to the robustness of the conclusion.

The ^{142}Nd evolution has commonly been interpreted to reflect early global differentiation followed by progressive remixing of an early differentiated reservoir, located at surface as continental crust or in the deep mantle (Caro et al., 2006; Bennett et al., 2007; Rizo

et al., 2012; Debaille et al., 2013; Roth et al., 2014). In this study, we have focused on the possibility of the former, but other interpretations are also possible (e.g., Morino et al., 2017). Geophysical considerations are usually brought up to evaluate the strengths and weaknesses of different interpretations, but we must bear in mind that our understanding of subsolidus mantle convection is still not sufficiently mature to allow its reliable extrapolation to early Earth conditions. For example, it is almost always assumed that mantle mixing in the early Earth was efficient because the mantle was hotter. Even though the mantle was most likely hotter in the past because of the secular cooling of the Earth (Herzberg et al., 2010), a hotter mantle does not necessarily imply more vigorous convection (e.g., Solomatov, 1996; Korenaga, 2011); mantle viscosity depends not only on temperature but also on grain size and water content. How a putative magma ocean might have solidified suffers from even greater uncertainties. Instead of extracting the continental crust, the formation of Mg-perovskite cumulates in a crystallizing magma ocean can also create a high Sm/Nd reservoir (Corgne et al., 2005), but the lower mantle could have solidified fully by equilibrium crystallization (Solomatov, 2015), under which elemental fractionation would not occur.

Given the current state of science in geodynamics, we have so far avoided to intermingle geodynamical speculations with geochemical interpretations. Our strategy is to first focus on modeling the Nd isotope evolution in the framework of continental growth and recycling, and then discuss the geophysical implications of modeling results. Unlike other possible interpretations, our interpretation of the Nd isotope evolution has an advantage of being supported quantitatively by two independent observations: (1) the present-day rate of sediment subduction, and (2) the present-day distribution of crust formation ages. Exploring its implications for early Earth geodynamics is thus of some merit. In doing so, it is important to recognize that to maintain zero net crustal growth after the Hadean (Fig. 1c) in the presence of intensive crustal recycling (Fig. 1d), the rate of new crustal generation has to match that of recycling. Therefore, even though the extremely rapid crustal growth in the early Hadean may in part reflect the solidification of the putative magma ocean, subsolidus mantle convection in the Archean must have been able to steadily produce the continental crust at the rate of $\sim 2 \times 10^{22}$ kg Gyr $^{-1}$ and then destroy it at a similar rate (cf. the rate of oceanic crust production in present-day plate tectonics is $\sim 7 \times 10^{22}$ kg Gyr $^{-1}$ Crisp, 1984). It is unclear whether such intensity of crustal evolution is compatible with stagnant lid convection or intermittent plate tectonics. A theoretical basis for intermittent plate tectonics in the early Earth has recently been shown to be questionable (Korenaga, 2017), and it would be more straightforward to explain our model of crustal evolution if plate tectonics was already operational in the early Earth (Hopkins et al., 2010).

In case of the continuous operation of plate tectonics throughout the Earth’s history, thermal evolution modeling suggests that average plate velocity in the past cannot be very different from the present-day value (Korenaga, 2011), and such thermal evolution is consistent with the cooling history of the upper mantle at least for the last 3.5 Gyr (Herzberg et al., 2010). Gradual decline in the rate of crustal generation may be explained by the secular cooling of the mantle, i.e., mantle melting was more extensive in the past, but the rate of crustal recycling has to decrease as well, which seems to be at odds with the relatively constant plate velocity through time. Its fourfold decrease over the Earth’s history (Fig. 1d) resembles the decay of internal heat generation (e.g., Turcotte and Schubert, 1982), but internal heat generation is not expected to manifest so directly in the tempo of tectonic processes, given our understanding of mantle convection in the Earth (Korenaga, 2016). Instead, the decline in crustal recycling may be explained by the greater preservation potential of continental crust, which can be

attained by the “cratonization” of continental crust (e.g., Cawood et al., 2013; Hawkesworth et al., 2017) or by the relative strengthening of continental mantle lithosphere owing to the hydration of convecting mantle (Korenaga, 2013). Even with the same tempo, the influence of plate tectonics on the surface environment could potentially be diverse because the physical and chemical state of the Earth’s interior has steadily been changing with time. Our understanding of such interaction between plate tectonics and the surface environment is still largely undeveloped.

Acknowledgements

This material is based upon work supported in part by the U.S. National Aeronautics and Space Administration through the NASA Astrobiology Institute under Cooperative Agreement No. NNA15BB03A issued through the Science Mission Directorate and by the U.S. National Science Foundation under grant EAR-1753916. The authors thank Stephen Mojzsis and Richard Carlson for a number of constructive comments and suggestions, which helped to improve the accuracy and clarity of the manuscript.

References

- Allegre, C.J., Hart, S.R., Minster, J.-F., 1983. Chemical structure and evolution of the mantle and continents determined by inversion of Nd and Sr isotopic data. II: numerical experiments and discussion. *Earth Planet. Sci. Lett.* 66, 191–213.
- Allegre, C.J., Lewin, E., 1995. Isotopic systems and stirring times of the Earth’s mantle. *Earth Planet. Sci. Lett.* 136, 629–646.
- Armstrong, R.L., 1981. Radiogenic isotopes: the case for crustal recycling on a near-steady-state no-continental-growth Earth. *Philos. Trans. R. Soc. Lond. A* 301, 443–472.
- Baadsgaard, H., Nutman, A.P., Bridgwater, D., 1986. Geochronology and isotopic variation of the early Archaean Amitsoq gneisses of the Isukasia area, southern West Greenland. *Geochim. Cosmochim. Acta* 50, 2173–2183.
- Barboni, M., Boehnke, P., Keller, B., Kohl, I.E., Schoene, B., Young, E.D., McKeegan, K.D., 2017. Early formation of the Moon 4.51 billion years ago. *Sci. Adv.* 3, e1602365.
- Bennett, V.C., 2003. Compositional evolution of the mantle. In: Holland, H.D., Turekian, K.K. (Eds.), *Treatise on Geochemistry*, vol. 2. Elsevier, pp. 493–519.
- Bennett, V.C., Brandon, A.D., Nutman, A.P., 2007. Coupled ^{142}Nd – ^{143}Nd isotopic evidence for Hadean mantle dynamics. *Science* 318, 1907–1910.
- Bouvier, A., Boyet, M., 2016. Primitive Solar System materials and Earth share a common initial ^{142}Nd abundance. *Nature* 537, 399–402.
- Bouvier, A., Vervoort, J.D., Patchett, P.J., 2008. The Lu–Hf and Sm–Nd isotopic composition of CHUR: constraints from unequilibrated chondrites and implications for the bulk composition of terrestrial planets. *Earth Planet. Sci. Lett.* 273, 48–57.
- Boyet, M., Carlson, R.W., 2005. ^{142}Nd evidence for early (>4.53 Ga) global differentiation of the silicate Earth. *Science* 309, 576–581.
- Bradley, D.C., 2008. Passive margins through earth history. *Earth-Sci. Rev.* 91, 1–26.
- Burkhardt, C., Borg, L.E., Brennecka, G.A., Shollenberger, Q.R., Dauphas, N., Kleine, T., 2016. A nucleosynthetic origin for the Earth’s anomalous ^{142}Nd composition. *Nature* 537, 394–398.
- Campbell, I.H., 2003. Constraints on continental growth models from Nb/U ratios in the 3.5 Ga Barberton and other Archaean basalt–komatiite suites. *Am. J. Sci.* 303, 319–351.
- Caro, G., Bourdon, B., Birck, J.-L., Moorbath, S., 2006. High-precision $^{142}\text{Nd}/^{144}\text{Nd}$ measurements in terrestrial rocks: constraints on the early differentiation of the Earth’s mantle. *Geochim. Cosmochim. Acta* 70, 164–191.
- Caro, G., Morino, P., Mojzsis, S.J., Cates, N.L., Bleeker, W., 2017. Sluggish Hadean geodynamics: evidence from coupled $^{146,147}\text{Sm}$ – $^{142,143}\text{Nd}$ systematics in Eoarchean supracrustal rocks of the Inukjuak domain (Québec). *Earth Planet. Sci. Lett.* 457, 23–37.
- Cawood, P.A., Hawkesworth, C.J., Dhuime, B., 2013. The continental record and the generation of continental crust. *GSA Bull.* 125, 14–32.
- Condie, K., Pisarevsky, S., Korenaga, J., Gardoll, S., 2015. Is the rate of supercontinent assembly changing with time? *Precambrian Res.* 259, 278–289.
- Corgne, A., Liebske, C., Wood, B.J., Rubie, D.C., Frost, D.J., 2005. Silicate perovskite–melt partitioning of trace elements and geochemical signature of a deep perovskite reservoir. *Geochim. Cosmochim. Acta* 69, 485–496.
- Crisp, J.A., 1984. Rates of magma emplacement and volcanic output. *J. Volcanol. Geotherm. Res.* 20, 177–211.
- Debaille, V., O’Neill, C., Brandon, A.D., Haenecour, P., Yin, Q.-Z., Mattioli, N., Treiman, A.H., 2013. Stagnant-lid tectonics in early Earth revealed by ^{142}Nd variations in late Archaean rocks. *Earth Planet. Sci. Lett.* 373, 83–92.
- DePaolo, D.J., 1980. Crustal growth and mantle evolution: inferences from models of element transport and Nd and Sr isotopes. *Geochim. Cosmochim. Acta* 44, 1185–1196.
- Goodwin, A.M., 1996. *Principles of Precambrian Geology*. Academic Press, London.
- Harrison, T.M., Blichert-Toft, J., Müller, W., Albareda, F., Holden, P., Mojzsis, S.J., 2005. Heterogeneous Hadean hafnium: evidence of continental crust at 4.4 to 4.5 Ga. *Science* 310, 1947–1950.
- Hawkesworth, C.J., Cawood, P.A., Dhuime, B., Kemp, A.I.S., 2017. Earth’s continental lithosphere through time. *Annu. Rev. Earth. Sci.* 45, 169–198.
- Herzberg, C., Condie, K., Korenaga, J., 2010. Thermal evolution of the Earth and its petrological expression. *Earth Planet. Sci. Lett.* 292, 79–88.
- Holland, H.D., 1984. *The Chemical Evolution of the Atmosphere and Oceans*. Princeton University Press.
- Hopkins, M.D., Harrison, T.M., Manning, C.E., 2010. Constraints on Hadean geodynamics from mineral inclusions in >4 Ga zircons. *Earth Planet. Sci. Lett.* 298, 367–376.
- Iizuka, T., Yamaguchi, T., Itano, K., Hibiya, Y., Suzuki, K., 2017. What Hf isotopes in zircon tell us about crust–mantle evolution. *Lithos* 274–275, 304–327.
- Jackson, M.G., Carlson, R.W., 2012. Homogeneous superchondritic $^{142}\text{Nd}/^{144}\text{Nd}$ in the mid-ocean ridge basalt and ocean island basalt mantle. *Geochim. Geophys. Geosyst.* 13, Q06011. <https://doi.org/10.1029/2012GC004114>.
- Jacobsen, S.B., Wasserburg, G.J., 1979. The mean age of mantle and crustal reservoirs. *J. Geophys. Res.* 84, 7411–7427.
- Jacobsen, S.B., Wasserburg, G.J., 1984. Sm–Nd isotopic evolution of chondrites and achondrites. II. *Earth Planet. Sci. Lett.* 67, 137–150.
- Jain, C., Korenaga, J., Karato, S., 2018. On the grain-size sensitivity of olivine rheology. *J. Geophys. Res., Solid Earth* 123, 674–688. <https://doi.org/10.1002/2017JB014847>.
- Korenaga, J., 2006. Archean geodynamics and the thermal evolution of Earth. In: Benn, K., Mareschal, J.-C., Condie, K. (Eds.), *Archean Geodynamics and Environments*. American Geophysical Union, Washington, D.C., pp. 7–32.
- Korenaga, J., 2009. A method to estimate the composition of the bulk silicate Earth in the presence of a hidden geochemical reservoir. *Geochim. Cosmochim. Acta* 73, 6952–6964.
- Korenaga, J., 2011. Thermal evolution with a hydrating mantle and the initiation of plate tectonics in the early Earth. *J. Geophys. Res.* 116, B12403. <https://doi.org/10.1029/2011JB008410>.
- Korenaga, J., 2013. Initiation and evolution of plate tectonics on Earth: theories and observations. *Annu. Rev. Earth Planet. Sci.* 41, 117–151.
- Korenaga, J., 2016. Can mantle convection be self-regulated? *Sci. Adv.* 2, e1601168.
- Korenaga, J., 2017. Pitfalls in modeling mantle convection with internal heating. *J. Geophys. Res., Solid Earth* 122, 4064–4085. <https://doi.org/10.1002/2016JB013850>.
- Korenaga, J., 2018. Estimating the formation age distribution of continental crust by unmixing zircon age data. *Earth Planet. Sci. Lett.* 482, 388–395.
- Korenaga, J., Karato, S., 2008. A new analysis of experimental data on olivine rheology. *J. Geophys. Res.* 113, B02403. <https://doi.org/10.1029/2007JB005100>.
- Korenaga, J., Planavsky, N.J., Evans, D.A.D., 2017. Global water cycle and the coevolution of Earth’s interior and surface environment. *Philos. Trans. R. Soc. Lond. A* 375, 20150393. <https://doi.org/10.1098/rsta.2015.0393>.
- Lyons, T.W., Reinhard, C.T., Planavsky, N.J., 2014. The rise of oxygen in Earth’s early ocean and atmosphere. *Nature* 506, 307–315.
- Lyubetskaya, T., Korenaga, J., 2007a. Chemical composition of Earth’s primitive mantle and its variance, 1: methods and results. *J. Geophys. Res.* 112, B03211. <https://doi.org/10.1029/2005JB004223>.
- Lyubetskaya, T., Korenaga, J., 2007b. Chemical composition of Earth’s primitive mantle and its variance, 2: implications for global geodynamics. *J. Geophys. Res.* 112, B03212. <https://doi.org/10.1029/2005JB004224>.
- Manga, M., 1996. Mixing of heterogeneities in the mantle: effect of viscosity differences. *Geophys. Res. Lett.* 23, 403–406.
- Marks, N., Borg, L., Hutcheon, I., Jacobsen, B., Clayton, R., 2014. Samarium–neodymium chronology and rubidium–strontium systematics of an Allende calcium–aluminum–rich inclusion with implications for ^{146}Sm half-life. *Earth Planet. Sci. Lett.* 405, 15–24.
- Matsumoto, M., Nishimura, T., 1998. Mersenne Twister: a 623-dimensionally equidistributed uniform pseudo-random number generator. *ACM Trans. Model. Comput. Simul.* 8, 3–30.
- McCulloch, M.T., Bennett, V.C., 1994. Progressive growth of the Earth’s continental crust and depleted mantle: geochemical constraints. *Geochim. Cosmochim. Acta* 58, 4717–4738.
- Mojzsis, S.J., Harrison, T.M., Pidgeon, R.T., 2001. Oxygen-isotope evidence from ancient zircons for liquid water at the Earth’s surface 4,300 Myr ago. *Nature* 409, 178–181.
- Moorbath, S., Whitehouse, M.J., Kamber, B.S., 1997. Extreme Nd-isotope heterogeneity in the early Archaean – fact or fiction? Case histories from northern Canada and West Greenland. *Chem. Geol.* 135, 213–231.
- Morino, P., Caro, G., Reisberg, L., Schmacher, A., 2017. Chemical stratification in the post-magma ocean Earth inferred from coupled $^{146,147}\text{Sm}$ – $^{142,143}\text{Nd}$ systematics in ultramafic rocks of the Saglek block (3.25–3.9 Ga, northern Labrador Canada). *Earth Planet. Sci. Lett.* 463, 136–150.

- Murphy, D.T., Brandon, A.D., Debaille, V., Burgess, R., Ballentine, C., 2010. In search of a hidden long-term isolated sub-chondritic $^{142}\text{Nd}/^{144}\text{Nd}$ reservoir in the deep mantle: implications for the Nd isotope systematics of the Earth. *Geochim. Cosmochim. Acta* 74, 738–750.
- O'Neil, J., Carlson, R.W., 2017. Building Archean cratons from Hadean mafic crust. *Science* 355, 1199–1202.
- O'Neil, J., Carlson, R.W., Paquette, J.-L., Francis, D., 2012. Formation age and metamorphic history of the Nuvvuagittuq greenstone belt. *Precambrian Res.* 220–221, 23–44.
- O'Neill, C., Debaille, V., 2014. The evolution of Hadean–Eoarchean geodynamics. *Earth Planet. Sci. Lett.* 406, 49–58.
- Padhi, C.M., Korenaga, J., Ozima, M., 2012. Thermal evolution of Earth with xenon degassing: a self-consistent approach. *Earth Planet. Sci. Lett.* 341–344, 1–9.
- Pehrsson, S.J., Eglinton, B.M., Evans, D.A.D., Huston, D., Reddy, S.M., 2016. Metallogeny and its link to orogenic style during the Nuna supercontinent cycle. In: Li, Z.-X., Evans, D.A.D., Murphy, J.B. (Eds.), *Supercontinent Cycles Through Earth History*. Geological Society of London, pp. 83–94.
- Puchtel, I.S., Touboul, M., Blichert-Toft, J., Walker, R.J., Bra, A.D., Nicklas, R.W., Kullik, V.K., Samsonov, A.V., 2016. Lithophile and siderophile element systematics of Earth's mantle at the Archean–Proterozoic boundary: evidence from 2.4 Ga komatiites. *Geochim. Cosmochim. Acta* 180, 227–255.
- Rizo, H., Boyet, M., Blichert-Toft, J., O'Neil, J., Rosing, M.T., Paquette, J.-L., 2012. The elusive Hadean enriched reservoir revealed by ^{142}Nd deficits in Isua Archaean rocks. *Nature* 491, 96–100.
- Roth, A.S.G., Bourdon, B., Mojzsis, S.J., Rudge, J.F., Guitreau, M., Blichert-Toft, J., 2014. Combined $^{147,146}\text{Sm}$ – $^{143,142}\text{Nd}$ constraints on the longevity and residence time of early terrestrial crust. *Geochem. Geophys. Geosyst.* 15, 2329–2345.
- Sanborn, M.E., Carlson, R.W., Wadhawa, M., 2015. $^{147,146}\text{Sm}$ – $^{143,142}\text{Nd}$, ^{176}Lu – ^{176}Hf , and ^{87}Rb – ^{87}Sr systematics in the angrites: implications for chronology and processes on the angrite parent body. *Geochim. Cosmochim. Acta* 171, 80–99.
- Scholl, D.W., von Huene, R., 2007. Crustal recycling at modern subduction zones applied to the past – issues of growth and preservation of continental basement, mantle geochemistry and supercontinent reconstruction. *Spec. Pap., Geol. Soc. Am.* 200, 9–32.
- Sleep, N.H., Zahnle, K.J., Lupu, R.E., 2014. Terrestrial aftermath of the Moon-forming impact. *Philos. Trans. R. Soc. Lond. A* 372, 20130172. <https://doi.org/10.1098/rsta.2013.0172>.
- Solomatov, V., 2015. *Magma Oceans and Primordial Mantle Differentiation*, 2nd ed. *Treatise on Geophysics*, vol. 9. Elsevier, pp. 81–104.
- Solomatov, V.S., 1996. Can hotter mantle have a larger viscosity? *Geophys. Res. Lett.* 23, 937–940.
- Stern, R.J., Scholl, D.W., 2010. Yin and yang of continental crust creation and destruction by plate tectonic processes. *Int. Geol. Rev.* 52, 1–31.
- Turcotte, D.L., Schubert, G., 1982. *Geodynamics: Applications of Continuum Physics to Geological Problems*. John Wiley, New York.
- Valley, J.W., Cavosie, A.J., Ushikubo, T., Reinhard, D.A., Lawrence, D.F., Larson, D.J., Clifton, P.H., Kelly, T.F., Wilde, S.A., Moser, D.E., Spicuzza, M.J., 2014. Hadean age for a post-magma-ocean zircon confirmed by atom-probe tomography. *Nat. Geosci.* 7, 219–223.
- Vervoort, J.D., Blichert-Toft, J., 1999. Evolution of the depleted mantle: Hf isotope evidence from juvenile rocks through time. *Geochim. Cosmochim. Acta* 63, 533–556.
- Wilde, S.A., Valley, J.W., Peck, W.H., Graham, C.M., 2001. Evidence from detrital zircons for the existence of continental crust and oceans on the Earth 4.4 Gyr ago. *Nature* 409, 175–178.
- Zindler, A., Hart, S., 1986. Chemical geodynamics. *Annu. Rev. Earth Planet. Sci.* 14, 493–571.